Horizontal and vertical seismic response of torsionally coupled buildings

R. K. Gupta

Department of Engineering, University of Tasmania, Launceston, Australia 7250

G. L. Hutchinson

Department of Civil and Environmental Engineering, University of Melbourne, Parkville, Australia 3052

(Received October 1992; revised version accepted January 1993)

Past analytical investigations have shown that the dynamic torsional coupling in asymmetric tall buildings, when subjected to the horizontal translational component of an earthquake, increases the response significantly. The effects of the vertical component of earthquake motion, acting simultaneously on the structure, are studied. A simple lumped-mass model of a single storey building resting on a rigid foundation has been developed and displacement responses are evaluated due to; firstly, horizontal motion; secondly, torsional motion; and thirdly, vertical motion. It has been concluded that the vertical response is very sensitive to the vertical frequency ratio (λ_v) values. For smaller λ_v values, the response is much higher when the translational natural period of uncoupled building (T_U) is greater than 1.2 s.

Keywords: seismic response, dynamic torsional coupling, asymmetric tall buildings

Tall buildings with eccentric centres of mass and resistance produce coupled lateral and torsional motions when subjected to the horizontal translational component of an earthquake. Analytical investigations of dynamic torsional coupling have concluded that its effects are most significant when translational and torsional natural frequencies of an equivalent uncoupled building are close, and that large torsional motions may be generated under such circumstances in buildings which are nominally symmetric. Most researchers have focused their attention on the horizontal component of ground motion and have failed to estimate the effects of the vertical component acting simultaneously on the structure. The rocking response of structures (produced by the vertical component) on elastic foundations are of major interest in soil-structure interaction.

This paper presents the development of a simple lumped-mass model of a single storey building with three degrees-of-freedom: firstly, the lateral displacement (u), secondly, the torsional displacement, u_θ; and thirdly, the vertical displacement, w. The building is assumed to be resting on a rigid foundation, and the mass (αm) of vertical elements (columns) of the building is lumped in line with the centre of resistance. The mass (m) of the diaphragm is acting at an eccentricity (e) from the centre of resistance.

In the analysis of earthquake response, it is assumed that the earthquake ground acceleration input in horizontal and vertical directions, $\ddot{u}_g(t)$ and $\ddot{w}_g(t)$, are applied uniformly over the base of the structure. The displacement responses due to the horizontal motion (u), the torsional motion (u_θ), the combined horizontal and torsional ($u + u_\theta$); and finally the vertical motion are evaluated in terms of the time history displacement for the El-Centro earthquake, N-S 1940, and for the Koyna, 1967 excitations. The calculations are carried out in the frequency domain employing the FFT technique to evaluate the transient responses. The complex frequency responses H_u, H_θ, $H_i(= H_u + H_\theta)$ and H_w are evaluated in discrete form from the solution of equations of motion. The derived earthquake responses depend on the structural parameters e_r, λ_T, λ_v, α and ζ together with the translational natural period T_U of the corresponding uncoupled mode, as well as the earthquake record itself. The damping ratio (ζ) is taken as 5% of the critical damping.

Notation

The following symbols are used in this paper:

a, b	Rayleigh's damping constants
c_{uu}, $c_{u\theta}$, $c_{\theta\theta}$, c_{ww}	coefficients of damping matrix

0141-0296/94/010011-14

C	damping matrix
C_i	generalized damping in mode i
CM, CR	centre of mass and centre of resistance of floor diaphragm, respectively
$C(\omega)$	Fourier transform of $p(t)$
D_{uu}, $D_{u\theta}$, $D_{\theta\theta}$, D_{ww}	dimensionless damping coefficients
e	structural eccentricity
e_r	eccentricity ratio (e/r)
f	normalized excitation frequency (ω/ω_1)
FFT	fast Fourier transform
g	acceleration due to gravity (9.81 m/s^2)
g(subscript)	ground motion quantity
h	storey height
H_i	complex frequency response of combined displacement at point i
H_u	complex frequency translational displacement response of floor
H_θ	complex frequency torsional displacement response of floor
H_w	complex frequency vertical displacement response of floor
$\boldsymbol{H}$	complex frequency response matrix
$H(\omega)$	response transfer function
$\|H_u\|$, $\|H_\theta\|$, $\|H_w\|$	system response amplitudes in x, θ and w directions, respectively
J_1, J_2	polar mass moment of inertia of floor mass and vertical structural elements (columns-lumped under centre of resistance)
k_u, k_θ, k_w	lateral, torsional and vertical storey stiffness, respectively
	mass of floor slab (disc)
max	maximum value of a response quantity
$\boldsymbol{M}$	mass matrix
$\boldsymbol{C}$	damping matrix
$\boldsymbol{K}$	stiffness matrix
M_i	generalized mass in mode i
n, k	integer counters in discrete Fourier transform summation
N	number of sample points employed in FFT computation
$p(t)$	loading function in time domain
P_{uu}, $P_{u\theta}$, $P_{\theta\theta}$, P_{ww}	complex coefficients in complex frequency response functions
r	radius of floor disc
R_i	coupled to uncoupled edge displacement ratio at i
t	time
T_o	loading period
T_U, T_W	translational and vertical uncoupled natural period, respectively
u, u_θ, w	time history of translational, torsional and vertical displacements of floor, respectively
u_i	combined response due to translation and rotation at point i
u_g, u_w	rigid base displacement in x and z directions, respectively
u, $\dot{u}$, $\ddot{u}$	time history of displacement, velocity and acceleration in lateral direction of building
u_θ, $\dot{u}_\theta$, $\ddot{u}_\theta$	time history of torsional displacement, torsional velocity and torsional acceleration of building, respectively
$\ddot{u}_g$, $\ddot{w}_g$	time history of earthquake ground acceleration records in horizontal and vertical directions, respectively
$\bar{u}$, $\bar{u}_\theta$, $\bar{w}$	amplitudes of translational, torsional and vertical displacements
$\bar{u}_i$	combined response amplitude at point i
$\bar{u}_g$, $\bar{w}_g$	ground displacement amplitudes in x and z directions, respectively
$\bar{\ddot{u}}_g$, $\bar{\ddot{w}}_g$	complex ground acceleration amplitudes
$\boldsymbol{u}$, $\dot{\boldsymbol{u}}$, $\ddot{\boldsymbol{u}}$	displacement, velocity and acceleration matrices, respectively
$\boldsymbol{u}_g$	ground motion matrix
w, $\dot{w}$, $\ddot{w}$	time history of displacement, velocity and acceleration in vertical direction, respectively
w_i	vertical response at point i
$\bar{w}_i$	vertical response amplitude at point i
W	exponential term ($= e^{\pm i2\pi/N}$)
x, y, z	Cartesian axes of reference (x, y horizontal)
$\boldsymbol{x}_0(k)$, $\boldsymbol{X}(n)$	discrete components for evaluation of FFT; n, $k = 0, 1, 2, \ldots N-1$
$\bar{X}_i$	resultant response at point i
α	ratio of mass of columns to mass of disc
ζ	viscous damping ratio, expressed as a fraction of critical damping
λ_T, λ_v	torsional and vertical frequency ratios, respectively
ω	excitation circular frequency
ω_n	natural frequency of torsionally coupled system ($n = 1, 2$)
ω_u, ω_θ, ω_w	translational, torsional and vertical natural frequencies, respectively
Ω_n	coupled natural frequency ratio (ω_n/ω_u)
ρ_a, ρ_b	mass densities of two halves of floor disc
φ_u, φ_θ, φ_w	harmonic response phase angles corresponding to responses u, u_θ and w, respectively

Structural system

A single storey building, shown in *Figure 1(a)*, consists of a rigid floor diaphragm of radius r supported on elastic columns. The total mass of the floor is represented by m and the mass of supporting columns is considered to be a fraction of the mass of the floor diaphragm, i.e., αm. The foundation of the building is assumed to be rigid.

The three degrees-of-freedom of the system are: the lateral displacement (u) of the centre of mass of the floor, relative to the ground, along the principal axis of resis-

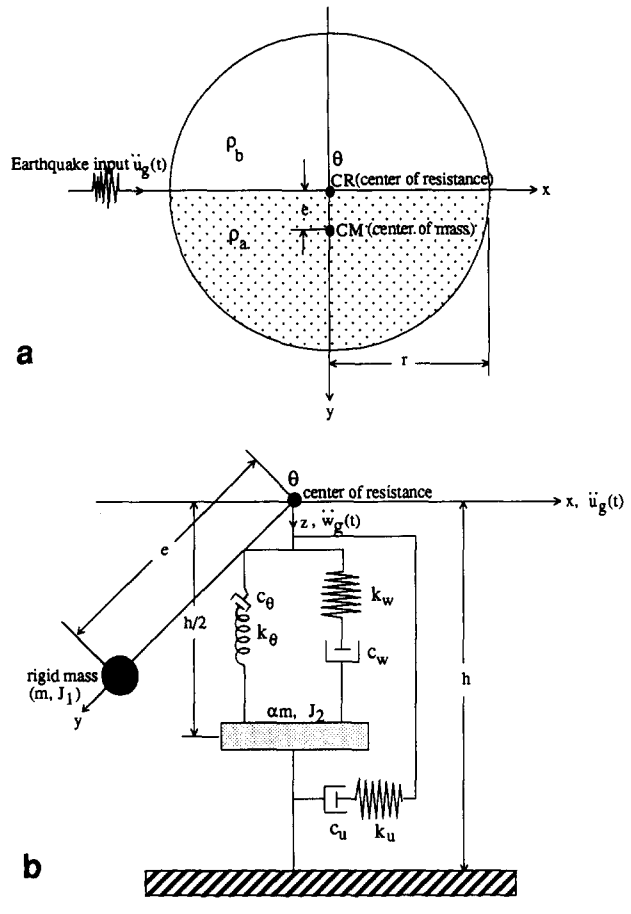

Figure 1 Lumped-mass model of single storey building

tance (x) of the building; the torsional displacement (u_θ) of the floor about the vertical axis (z); and the vertical displacement (w) of the centre of mass of the supporting columns, relative to the ground, along the principal axis of resistance (z) of the building. In this paper the centres of mass of the supporting columns are assumed to be in line with the principal axis of resistance. The response displacements of the floor diaphragm are assumed to be sufficiently small to ensure the structural stability and, therefore, the effects of changes in the geometry may be neglected.

Lumped-mass model

The vertical elements (columns) are considered to be elastic of mass αm, where α represents the fraction of floor mass m. Their combined lateral and torsional interstorey stiffnesses are idealized by massless, elastic, and viscously damped springs (*Figure 1(b)*). Furthermore, a symmetrical distribution of the lateral stiffness is assumed, such that the centre of resistance coincides with the centre of the floor (disc). The structural eccentricity (e), between the centres of mass and resistance perpendicular to the loading direction (x) is caused by different mass densities (ρ_a, ρ_b; $\rho_a > \rho_a$) in the two halves of the floor disc, split along $y = 0$, as shown in *Figure 1(a)*. The principal axes of resistance coincide with the x and y horizontal axes of the reference system. The principal axis of resistance in the vertical direction coincides with the z axis of the reference system. The rotational displacement (θ) of the disc takes place about the centre of resistance ($x = y = 0$).

Ground motion input

In order to establish the frequency domain solution to the equations of motion, the ground excitation is assumed to be applied as a harmonic, rigid-base displacements u_g and w_g in the x and z directions, respectively.

$$u_g = \bar{u}_g e^{i\omega t}$$
$$w_g = \bar{w}_g e^{i\omega t} \tag{1}$$

where ω is the circular frequency of excitation, $\bar{u}_g$ and $\bar{w}_g$ represent the ground displacement amplitudes.

Equations of motion

The equations of motion of the building model (*Figure 1*) are derived from the dynamic equilibrium for each degree-of-freedom.

x-direction

$$m\ddot{u} + me\ddot{\theta} + c_{uu}\dot{u} + c_{u\theta}\dot{\theta} + k_u u = -m\ddot{u}_g \tag{2}$$

θ-direction

$$(J_1 + J_2)\ddot{\theta} + me\ddot{u} + c_{u\theta}\dot{u} + c_{\theta\theta}\dot{\theta} + k_\theta\theta = -me\ddot{u}_g \tag{3}$$

z-direction

$$\alpha m\ddot{w} + c_{ww}\dot{w} + k_w w = -\alpha m\ddot{w}_g \tag{4}$$

Substituting $u_\theta = r\theta$; $e_r = e/r$; $J_1 = mr^2/2$; $J_2 = \alpha mr^2/2$, and writing equations (2-4) in matrix form we obtain

$$\underbrace{\begin{bmatrix} 1 & e_r & 0 \\ e_r & \frac{1+\alpha}{2} & 0 \\ 0 & 0 & \alpha \end{bmatrix}}_{[M]} \begin{Bmatrix} \ddot{u} \\ \ddot{u}_\theta \\ \ddot{w} \end{Bmatrix} + \underbrace{\begin{bmatrix} \frac{c_{uu}}{m} & \frac{c_{u\theta}}{mr} & 0 \\ \frac{c_{u\theta}}{mr} & \frac{c_{\theta\theta}}{mr^2} & 0 \\ 0 & 0 & \frac{c_{ww}}{m} \end{bmatrix}}_{[C]} \begin{Bmatrix} \dot{u} \\ \dot{u}_\theta \\ \dot{w} \end{Bmatrix}$$
$$+ \underbrace{\begin{bmatrix} \frac{k_u}{m} & 0 & 0 \\ 0 & \frac{k_\theta}{mr^2} & 0 \\ 0 & 0 & \frac{k_w}{m} \end{bmatrix}}_{[K]} \begin{Bmatrix} u \\ u_\theta \\ w \end{Bmatrix} = - \underbrace{\begin{Bmatrix} \ddot{u}_g \\ e_r\ddot{u}_g \\ \alpha\ddot{w}_g \end{Bmatrix}}_{[u_g]} \tag{5}$$

where $[M]$, $[C]$, $[K]$, and $[u_g]$ are the mass, damping, stiffness, and ground motion matrices, respectively.

It should be noted that the mass of the columns is considered to have insignificant influence on the horizontal response, and is therefore ignored in equations (2) and (3). The mass of the diaphragm is ignored in equation (4) to avoid creating eccentricity in the vertical direction. This assumption will influence the natural period of vertical vibrations which may further enhance the vertical response.

Evaluation of damping matrix coefficients

$$C = a[M] + b[K] \tag{6}$$

a and b are arbitrary proportionality factors and are determined by assuming that both the natural modes of vibration (u and u_θ) of the coupled system have the same

ratio ζ of critical damping. The damping matrix proportional to the mass and/or stiffness matrices will permit uncoupling the equations of motion. For each mode the generalized damping is given by

$$C_i = \Phi_i^T \boldsymbol{C} \Phi_i = 2\zeta_i \omega_i M_i$$
$$C_i = \Phi_i^T \boldsymbol{C} \Phi_j = 0 \quad i \neq j \tag{7}$$

where ω_i is the natural frequency of the coupled system in mode i, M_i is the generalized mass in mode i, and ζ is the modal damping ratio.

$$\Phi_i^T (a\boldsymbol{M} + b\boldsymbol{K}) \Phi_i = 2\zeta_i \omega_i M_i$$
$$a\Phi_i^T \boldsymbol{M} \Phi_i + b\Phi_i^T \boldsymbol{K} \Phi_i = 2\zeta_i \omega_i M_i$$
$$aM_i + bK_i = 2\zeta_i \omega_i M_i$$
$$aM_i + bM_i \omega_i^2 = 2\zeta_i \omega_i M_i \left(\text{since } \omega_i^2 = \frac{K_i}{M_i}\right)$$
$$a + b\omega_i^2 = 2\zeta_i \omega_i \; i = 1, 2 \tag{8}$$

Solving the equations in (8) yields

$$a = \frac{2\zeta\omega_1\omega_2}{\omega_1 + \omega_2} \quad b = \frac{2\zeta}{\omega_1 + \omega_2} \tag{9}$$

where ω_1 and ω_2 are the fundamental and secondary natural frequencies of the coupled system. Substituting a and b into equation (6) yields

$$C = \frac{2\zeta\omega_1\omega_2}{\omega_1 + \omega_2} \begin{bmatrix} 1 & e_r & 0 \\ e_r & \frac{1+\alpha}{2} & 0 \\ 0 & 0 & \alpha \end{bmatrix} + \frac{2\zeta}{\omega_1 + \omega_2} \begin{bmatrix} \frac{k_u}{m} & 0 & 0 \\ 0 & \frac{k_\theta}{mr^2} & 0 \\ 0 & 0 & \frac{k_w}{m} \end{bmatrix} \tag{10}$$

Comparing equations (10) and (5)

$$\frac{C_{uu}}{m} = \frac{2\zeta\omega_1\omega_2}{\omega_1 + \omega_2} + \frac{2\zeta k_u}{\omega_1 + \omega_2}$$
$$\frac{C_{u\theta}}{mr} = \frac{C_{\theta u}}{mr} = \frac{2\zeta\omega_1\omega_2}{\omega_1 + \omega_2} e_r$$
$$\frac{C_{\theta\theta}}{mr^2} = \frac{2\zeta\omega_1\omega_2}{\omega_1 + \omega_2} \frac{1+\alpha}{2} + \frac{2\zeta}{\omega_1 + \omega_2} \frac{k_\theta}{mr^2}$$
$$\frac{C_{ww}}{m} = \frac{2\zeta\omega_1\omega_2}{\omega_1 + \omega_2} \alpha + \frac{2\zeta}{\omega_1 + \omega_2} \frac{k_w}{m} \tag{11}$$

Let ω_u and ω_θ represent the translational and torsional natural frequencies, respectively, of the corresponding torsionally uncoupled building (zero eccentricity), and let ω_w denote the vertical natural frequency, then

$$k_u = m\omega_u^2$$
$$k_\theta = (J_1 + J_2)\omega_\theta^2 = \frac{1+\alpha}{2} mr^2 \omega_\theta^2$$
$$k_w = \alpha m \omega_w^2$$

Defining

$$\lambda_T = \frac{\omega_\theta}{\omega_u} \quad \lambda_v = \frac{\omega_w}{\omega_u} \quad \Omega_n = \frac{\omega_n}{\omega_u} \quad (n = 1, 2)$$

From equation (11)

$$C_{uu} = \frac{2\zeta\omega_1\omega_2}{\omega_1 + \omega_2} + \frac{2\zeta m\omega_u^2}{\omega_1 + \omega_2}$$
$$= 2\zeta m\omega_1 \left[\frac{1}{\Omega_1 + \Omega_2}\right]\left[\Omega_2 + \frac{1}{\Omega_1}\right]$$
$$\left(\text{since } \omega_u^2 = \frac{\omega_1\omega_2}{\Omega_1\Omega_2}\right) = 2\zeta m\omega_1 D_{uu} \tag{12}$$

Similarly

$$C_{u\theta} = \frac{2\zeta\omega_1\omega_2}{\omega_1 + \omega_2} mr = 2\zeta\omega_1 me \left[\frac{\Omega_2}{\Omega_1 + \Omega_2}\right]$$
$$= 2\zeta\omega_1 me D_{u\theta} \tag{13}$$
$$C_{\theta\theta} = \frac{2\zeta\omega_1\omega_2}{\omega_1 + \omega_2} \frac{(1+\alpha)}{2} mr^2 + \frac{2\zeta k_\theta}{\omega_1 + \omega_2}$$
$$= 2\zeta \frac{(1+\alpha)}{2} mr^2 \left[\frac{\omega_1\omega_2}{\omega_1 + \omega_2} + \frac{\omega_\theta^2}{\omega_1 + \omega_2}\right]$$
$$= 2\zeta\omega_1 \frac{(1+\alpha)}{2} mr^2 \left[\frac{1}{\Omega_1 + \Omega_2}\right]\left[\Omega_2 + \frac{\lambda_T^2}{\Omega_1}\right]$$
$$= 2\zeta\omega_1 \frac{(1+\alpha)}{2} mr^2 D_{\theta\theta} \tag{14}$$
$$C_{ww} = \frac{2\zeta\omega_1\omega_2}{\omega_1 + \omega_2} \alpha m + \frac{2\zeta m\alpha\omega_w^2}{\omega_1 + \omega_2}$$
$$= 2\zeta m\alpha \left[\frac{\omega_1\omega_2}{\omega_1 + \omega_2}\right]\left[1 + \frac{\lambda_v^2\omega_u^2}{\omega_1\omega_2}\right]$$
$$= 2\zeta m\alpha\omega_1 \left[\frac{\Omega_2}{\Omega_1 + \Omega_2}\right]\left[1 + \frac{\lambda_v^2}{\Omega_1\Omega_2}\right]$$
$$= 2\zeta m\alpha\omega_1 D_{ww} \tag{15}$$

where

$$D_{uu} = \left[\frac{1}{\Omega_1 + \Omega_2}\right]\left[\Omega_2 + \frac{1}{\Omega_1}\right]$$
$$D_{u\theta} = \left[\frac{\Omega_2}{\Omega_1 + \Omega_2}\right] \tag{16}$$
$$D_{\theta\theta} = \left[\frac{1}{\Omega_1 + \Omega_2}\right]\left[\Omega_2 + \frac{\lambda_T^2}{\Omega_1}\right]$$
$$D_{ww} = \left[\frac{1}{\Omega_1 + \Omega_2}\right]\left[\Omega_2 + \frac{\lambda_v^2}{\Omega_1}\right]$$

Natural frequencies

The undamped natural frequencies of the system are determined from the free vibration solution of the follow-

ing

$$\begin{bmatrix} 1 & e_r & 0 \\ e_r & \dfrac{1+\alpha}{2} & 0 \\ 0 & 0 & \alpha \end{bmatrix} \begin{Bmatrix} \ddot{u} \\ \ddot{u}_\theta \\ \ddot{w} \end{Bmatrix} + \begin{bmatrix} \dfrac{k_u}{m} & 0 & 0 \\ 0 & \dfrac{k_\theta}{mr^2} & 0 \\ 0 & 0 & \dfrac{k_w}{m} \end{bmatrix} \begin{Bmatrix} u \\ u_\theta \\ w \end{Bmatrix} = \begin{Bmatrix} 0 \\ 0 \\ 0 \end{Bmatrix} \quad (17)$$

Since

$$\frac{k_u}{m} = \omega_u^2 = \frac{\omega_1^2}{\Omega_1^2}$$

$$\frac{k_\theta}{mr^2} = \frac{(1+\alpha)}{2}\omega_\theta^2 = \frac{(1+\alpha)}{2}\lambda_T^2\omega_u^2 = \frac{(1+\alpha)}{2}\lambda_T^2\frac{\omega_1^2}{\Omega_1^2}$$

$$\frac{k_w}{m} = \alpha\omega_w^2 = \alpha\lambda_v^2\omega_v^2 = \alpha\lambda_v^2\frac{\omega_1^2}{\Omega_1^2}$$

Equation (17) becomes

$$\begin{bmatrix} 1 & e_r & 0 \\ e_r & \dfrac{1+\alpha}{2} & 0 \\ 0 & 0 & \alpha \end{bmatrix} \begin{Bmatrix} \ddot{u} \\ \ddot{u}_\theta \\ \ddot{w} \end{Bmatrix} + \frac{\omega_1^2}{\Omega_1^2} \begin{bmatrix} 1 & 0 & 0 \\ 0 & \dfrac{(1+\alpha)}{2}\lambda_T^2 & 0 \\ 0 & 0 & \alpha\lambda_v^2 \end{bmatrix} \begin{Bmatrix} u \\ u_\theta \\ w \end{Bmatrix} = \begin{Bmatrix} 0 \\ 0 \\ 0 \end{Bmatrix} \quad (18)$$

For harmonic ground motion,
$u_g = \bar{u}_g e^{i\omega t}$, the steady state response is given by

$$\boldsymbol{u} = \begin{Bmatrix} u \\ u_\theta \\ w \end{Bmatrix} = \begin{Bmatrix} H_u \\ H_\theta \\ H_w \end{Bmatrix} e^{i\omega t} = \boldsymbol{H} e^{i\omega t}$$

where H_u, H_θ, and H_w are the complex frequency response functions defining the response u, u_θ, and w, respectively. From equation (19)

$$\ddot{\boldsymbol{u}} = -\omega^2 \boldsymbol{H} e^{i\omega t} \quad (20)$$

Equation (17) may then be written as

$$\omega^2 e^{i\omega t} \begin{bmatrix} 1 & e_r & 0 \\ e_r & \dfrac{1+\alpha}{2} & 0 \\ 0 & 0 & \alpha \end{bmatrix} \begin{Bmatrix} H_u \\ H_\theta \\ H_w \end{Bmatrix} - \frac{\omega_1^2}{\Omega_1^2} e^{i\omega t} \begin{bmatrix} 1 & 0 & 0 \\ 0 & \dfrac{(1+\alpha)}{2}\lambda_T^2 & 0 \\ 0 & 0 & \alpha\lambda_v^2 \end{bmatrix} \begin{Bmatrix} H_u \\ H_\theta \\ H_w \end{Bmatrix} = \begin{Bmatrix} 0 \\ 0 \\ 0 \end{Bmatrix} \quad (21)$$

The frequency determinant may be written by simplifying the above as

$$\begin{vmatrix} \left(\dfrac{\omega_1^2}{\Omega_1^2} - \omega^2\right) & -e_r\omega^2 & 0 & 0 & 0 \\ -e_r\omega^2 & \left(\dfrac{\omega_1^2}{\Omega_1^2}\dfrac{(1+\alpha)}{2}\lambda_T^2 - \dfrac{(1+\alpha)}{2}\omega^2\right) & 0 & 0 & 0 \\ 0 & 0 & \left(\dfrac{\omega_1^2}{\Omega_1^2}\alpha\lambda_v^2\right) - \omega^2\alpha \end{vmatrix} = 0 \quad (22)$$

Steady state response

The steady state displacement and acceleration responses ($\dot{\boldsymbol{u}}$ and $\ddot{\boldsymbol{u}}$) are given by equations (19) and (20), respectively. The corresponding steady state velocity response is obtained from equation (19) as

$$\dot{\boldsymbol{u}} = i\omega \boldsymbol{H} e^{i\omega t} \quad (23)$$

Substituting equations (19, 20 and 23) into equation (5) and simplifying yields

$$-\omega^2 \begin{bmatrix} 1 & e_r & 0 \\ e_r & \dfrac{(1+\alpha)}{2} & 0 \\ 0 & 0 & \alpha \end{bmatrix} + 2i\zeta\omega\omega_1 \begin{bmatrix} D_{uu} & e_r D_{u\theta} & 0 \\ e_r D_{u\theta} & \dfrac{(1+\alpha)}{2} D_{\theta\theta} & 0 \\ 0 & 0 & \alpha D_{ww} \end{bmatrix} + \frac{\omega_1^2}{\Omega_1^2} \begin{bmatrix} 1 & 0 & 0 \\ 0 & \dfrac{(1+\alpha)}{2}\lambda_T^2 & 0 \\ 0 & 0 & \alpha\lambda_v^2 \end{bmatrix} \begin{Bmatrix} H_u \\ H_\theta \\ H_w \end{Bmatrix} = \omega^2 \begin{Bmatrix} \bar{u}_g \\ e_r\bar{u}_g \\ \alpha\bar{w}_g \end{Bmatrix} \quad (24)$$

Writing the normalized excitation frequency, $f = \omega/\omega_1$, and dividing both sides by ω_1^2 gives

$$\frac{1}{\Omega_1^2} \begin{bmatrix} 1 & 0 & 0 \\ 0 & \dfrac{(1+\alpha)}{2}\lambda_T^2 & 0 \\ 0 & 0 & \alpha\lambda_v^2 \end{bmatrix} - f^2 \begin{bmatrix} 1 & e_r & 0 \\ e_r & \dfrac{(1+\alpha)}{2} & 0 \\ 0 & 0 & \alpha \end{bmatrix} + 2i\zeta f \begin{bmatrix} D_{uu} & e_r D_{u\theta} & 0 \\ e_r D_{u\theta} & \dfrac{(1+\alpha)}{2} D_{\theta\theta} & 0 \\ 0 & 0 & \alpha D_{ww} \end{bmatrix} \begin{Bmatrix} \dfrac{H_u}{\bar{u}_g} \\ \dfrac{H_\theta}{\bar{u}_g} \\ \dfrac{H_w}{\bar{u}_g} \end{Bmatrix} = f^2 \begin{Bmatrix} 1 \\ e_r \\ \alpha \end{Bmatrix} \quad (25)$$

It may be seen that the response parameters $H_u/\bar{u}_g$, $H_\theta/\bar{u}_g$ and $H_w/\bar{u}_g$ depend only on e_r, α, ζ, λ_T, λ_v and f. The first five parameters define the structural system, while the sixth (f) together with the amplitudes $\bar{u}_g$ and $\bar{w}_g$ define the ground motion. The solution of the simultaneous linear algebraic equations (25) is given below which yields the system's response amplitudes $\bar{u}/\bar{u}_g$, $\bar{u}_\theta/\bar{u}_g$, and $\bar{w}/\bar{w}_g$ and the corresponding phase angle φ_u, φ_θ and φ_w. It should be noted that

$$\bar{u} = \|H_u\|,\ \bar{u}_\theta = \|H_\theta\|,\ \bar{w} = \|H_w\| \tag{26}$$

Expanding equations (25) yields

$$\left[\frac{1}{\Omega_1^2} - f^2 + 2i\zeta D_{uu}\right]\frac{H_u}{\bar{u}_g} + [-f^2 e_r + 2i\zeta f e_r D_{u\theta}]\frac{H_\theta}{\bar{u}_g} = f^2$$

$$[-f^2 e_r + 2i\zeta f e_r D_{u\theta}]\frac{H_u}{\bar{u}_g} + \left[\frac{1}{\Omega_1^2}\frac{(1+\alpha)}{2}\lambda_T^2 - f^2\frac{(1+\alpha)}{2} + 2i\zeta f\frac{(1+\alpha)}{2}D_{\theta\theta}\right] \times \frac{H_\theta}{\bar{u}_g} = f^2 e_r$$

$$\times\left[\frac{1}{\Omega_1^2}\lambda_v^2 - f^2 + 2i\zeta f D_{ww}\right]\frac{H_w}{\bar{w}_g} = f^2 \tag{27}$$

Equations (27) may be summarized as

$$P_{uu}\left(\frac{H_u}{\bar{u}_g}\right) + P_{u\theta}\left(\frac{H_\theta}{\bar{u}_g}\right) = f^2$$

$$P_{u\theta}\left(\frac{H_u}{\bar{u}_g}\right) + P_{\theta\theta}\left(\frac{H_\theta}{\bar{u}_g}\right) = f^2 e_r$$

$$P_{ww}\left(\frac{H_w}{\bar{w}_g}\right) = f^2 \tag{28}$$

where P_{uu}, $P_{u\theta}$, $P_{\theta\theta}$ and P_{ww} are complex coefficients given by

$$P_{uu} = R_1 + iI_1;\ P_{u\theta} = R_2 + iI_2$$
$$P_{\theta\theta} = R_3 + iI_3;\ P_{ww} = R_4 + iI_4 \tag{29}$$

where

$$R_1 = \frac{1}{\Omega_1^2} - f^2;\ I_1 = 2\zeta f D_{uu}$$
$$R_2 = -f^2 e_r;\ I_2 = 2\zeta f e_r D_{u\theta}$$
$$R_3 = \frac{1(1+\alpha)}{\Omega_1^2\, 2}\lambda_T^2 - f^2\frac{(1+\alpha)}{2};\ I_3 = 2\zeta f\frac{(1+\alpha)}{2}D_{\theta\theta}$$
$$R_4 = \frac{1(1+\alpha)}{\Omega_1^2\, 2}\lambda_v^2 - f^2;\ I_4 = 2\zeta f D_{ww} \tag{30}$$

Solving equations (28), simultaneously, yields

$$\frac{H_u}{\bar{u}_g} = \frac{f^2(e_r P_{u\theta} - P_{\theta\theta})}{P_{u\theta}^2 - P_{uu}P_{\theta\theta}} \tag{31a}$$

$$\frac{H_\theta}{\bar{u}_g} = \frac{f^2(P_{u\theta} - e_r P_{uu})}{P_{u\theta}^2 - P_{uu}P_{\theta\theta}} \tag{31b}$$

$$\frac{H_w}{\bar{u}_g} = \frac{f^2}{P_{ww}} \tag{31c}$$

where the numerators and the common denominator in equations (31(a) and 31(b)) may be written as

$$f^2[e_r(R_2 + iI_2) - (R_3 + iI_3)] = R_5 + iI_5 \tag{32a}$$
$$f^2[(R_2 + iI_2) - e_r(R_1 + iI_1)] = R_6 + iI_6 \tag{32b}$$
$$[(R_2 + iI_2)^2 - (R_1 + iI_1)(R_3 + iI_3)] = R_7 + iI_7 \tag{32c}$$

where

$$R_5 = f^2(e_r R_2 - R_3);\ I_5 = f^2(e_r I_2 - I_3)$$
$$R_6 = f^2(R_2 - e_r R_1);\ I_6 = f^2(I_2 - e_r I_1)$$
$$R_7 = R_2^2 - I_2^2 - R_1 R_3 + I_1 I_3$$
$$I_7 = 2R_2^2 I_2^2 - R_3 I_1 - R_1 I_3$$

Using equations (32), equations (31) are written as

$$\frac{H_u}{\bar{u}_g} = \frac{R_5 + iI_5}{R_7 + iI_7} = R_8 + iI_8$$
$$\frac{H_\theta}{\bar{u}_g} = \frac{R_6 + iI_6}{R_7 + iI_7} = R_9 + iI_9$$
$$\frac{H_w}{\bar{u}_g} = \frac{f^2}{R_4 + iI_4} = R_{10} + iI_{10}$$

where

$$R_8 = \frac{R_5 R_7 + I_5 I_7}{R_7^2 + I_7^2}$$
$$I_8 = \frac{R_7 I_5 - R_5 I_7}{R_7^2 + I_7^2}$$
$$R_9 = \frac{R_6 R_7 + I_6 I_7}{R_7^2 + I_7^2}$$
$$R_{10} = \frac{f^2 R_4}{R_4^2 + I_4^2}$$
$$I_{10} = -\frac{f^2 I_4}{R_4^2 + I_4^2} \tag{35}$$

The response amplitudes $\|H_u\|$, $\|H_\theta\|$, and $\|H_w\|$, normalized to the ground amplitude $\bar{u}_g$, $\bar{u}_g$ and $\bar{w}_g$, respectively, and the corresponding phase angles φ_u, φ_θ and φ_w may be written using equations (34) as

$$\frac{\|H_u\|}{\bar{u}_g} = (R_8^2 + I_8^2)^{1/2} = \frac{\bar{u}}{\bar{u}_g}$$
$$\frac{\|H_\theta\|}{\bar{u}_g} = (R_9^2 + I_9^2)^{1/2} = \frac{\bar{u}_\theta}{\bar{u}_g}$$
$$\frac{\|H_w\|}{\bar{w}_g} = (R_{10}^2 + I_{10}^2)^{1/2} = \frac{\bar{w}}{\bar{w}_g} \tag{36}$$

and

$$\varphi_u = \tan^{-1}(I_8/R_8);\ \varphi_\theta = \tan^{-1}(I_9/R_9)$$
$$\varphi_w = \tan^{-1}(I_{10}/R_{10}) \tag{37}$$

From equation (19), the variation of the loading and response terms u_g, u, u_θ and w is obtained by taking the

projections of the relevant vectors onto the real axis, i.e.

$$u = H_u e^{i\omega t} = \|H_u\| e^{-i\varphi_u} e^{i\omega t} = \|H_u\| e^{i(\omega t - \varphi_u)}$$
$$u_\theta = H_\theta e^{i\omega t} = \|H_\theta\| e^{i(\omega t - \varphi_\theta)}$$
$$w = H_w e^{i\omega t} = \|H_w\| e^{i(\omega t - \varphi_w)} \quad (38)$$

The quantities φ_u, φ_θ, φ_w are defined as the phase angles by which the responses u, u_θ and w lag behind the applied loading u_g, u_g and w_g, respectively.

Horizontal response

The combined effect of translation (u) and rotation (u_θ) responses at point 'i' is

$$u_i = u + u_\theta$$

$$u_i = H_i e^{i\omega t} = H_u e^{i\omega t} + H_\theta e^{i\omega t} = (H_u + H_\theta) e^{i\omega t} \quad (40)$$

The complex transfer functions, H_i, normalized to the ground amplitude, $\bar{u}_g$, is given by

$$\frac{H_i}{\bar{u}_g} = \frac{H_u + H_\theta}{\bar{u}_g} \quad (41)$$

The complex transfer functions, H_i, corresponding to the combined response, u_i, is expressed in amplitude-phase form as

$$H_i = \|H_i\| e^{-i\varphi_i} = \bar{u}_i e^{-i\varphi_i} \quad (42)$$

where $\bar{u}_i$ is the response amplitude and φ_i is the phase angle by which the response, u_i, lags behind the applied ground excitation (u_g). From equations (34) and (41),

$$H_i/\bar{u}_g = (R_8 + R_9) + i(I_8 + I_9) \quad (43)$$

The response amplitude, u_i, and the phase angle, φ_i, are calculated from equations (43), i.e.,

$$\bar{u}_i/\bar{u}_g = \|H_i\|/\bar{u}_g = [(R_8 + R_9)^2 + (I_8 + I_9)^2]^{1/2}$$
$$\varphi_i = \tan^{-1}[(I_8 + I_9)/(R_8 + R_9)]$$

Vertical response

$$w_i = H_i e^{i\omega t} = H_w e^{i\omega t} \quad (45)$$
$$H_i/\bar{w}_g = H_w/\bar{w}_g \quad (46)$$
$$H_i = \|H_i\| e^{-i\varphi_i} = \bar{w}_i e^{-i\varphi_i} \quad (47)$$

where $\bar{w}_i$ is the response amplitude and φ_i is the phase angle by which the response, w_i, lags behind the applied ground acceleration (w_g). From equations (34) and (46)

$$H_i/\bar{w}_g = R_{10} + iI_{10}$$
$$\bar{w}_i/\bar{w}_g = \|H_i\|/\bar{w}_g = [R_{10}^2 + I_{10}^2]^{1/2}$$
$$\varphi_i = \tan^{-1}[(I_{10}/R_{10})] \quad (48)$$

Resultant response

The resultant response at point 'i' is calculated as

$$\bar{X}_i = [(\bar{u}_i/\bar{u}_g)^2 + (\bar{w}_i/\bar{w}_g{}^2]^{1/2}$$
$$= [(R_8 + R_9)^2 + R_{10}^2 + (I_8 + I_9)^2 + I_{10}^2]^{1/2} \quad (49)$$
$$\bar{\Phi}_i = \tan^{-1}[(R_{10}^2 + I_{10}^2)^{1/2}/\{(R_8 + R_9)^2 + (I_8 + I_9)^2\}] \quad (50)$$

Earthquake response using fast Fourier transform (FFT)

The horizontal and vertical components of earthquake ground acceleration input, $\ddot{u}_g$ and $\ddot{w}_g$ are assumed to be applied uniformly over the rigid base of the structure so that interaction effects can be neglected. Each response is expressed in terms of a time-history displacement for a particular earthquake excitation. The chosen earthquake records are expressed in terms of digitized ground acceleration data, corrected according to Schiff and Bodganoff[1].

The theory of the fast Fourier transform (FFT) technique has been well covered in the literature, both for general applications[2] and for algorithms developed for use in structural dynamics[3]. For frequency-domain calculations, the relationship between the time-domain loading function $p(t)$ and its frequency - domain counterpart $c(\omega)$, known as its Fourier transform, is given by

$$c(\omega) = \int_{t=-\infty}^{\infty} p(t)\exp(-i\omega t)\,dt \quad (51)$$

To apply this frequency-domain procedure, it is necessary to evaluate the harmonic components $c(\omega)$ by taking the forward Fourier transform of the given loading using equation (51), and then introducing an appropriate response transfer function $H(\omega)$ before finally inversing the Fourier transform procedure by employing the following equation

$$u(t) = \frac{1}{2\pi}\int_{\omega=-\infty}^{\infty} H(\omega)c(\omega)\exp(i\omega t)\,d\omega \quad (52)$$

The basic equation to be employed in evaluating both the forward and inverse transform in discrete form[3] is represented by

$$X(n) = \sum_{k=0}^{N-1} x_o(k)W^{nk} \quad n = 0, 1, 2, \ldots N-1 \quad (53)$$

Where the exponential term $W = e^{\pm i2\pi/N}$, and N is the number of sample points taken from the loading record over a loading period T_o ($> D$, where D is the load duration). The modified FFT algorithm[3] has been used to evaluate transient response (time-history) $u(t)$, $u_\theta(t)$, $w(t)$ and $u_i(t)$ using the Fourier transform technique requires the use of the corresponding complex frequency response functions H_u, H_θ, H_w and H_i. These have been evaluated in the preceding sections as functions of the system parameters e_r, α, ζ, λ_T, λ_v and f, where the complex transfer functions are normalized to $\bar{u}_g$ and $\bar{w}_g$ appropriately (the ground excitation amplitudes). Differentiating equations (1) yield

$$\ddot{u}_g = -\omega^2 \bar{u}_g e^{i\omega t} = \bar{\bar{u}}_g e^{i\omega t}$$
$$\ddot{w}_g = -\omega^2 \bar{w}_g e^{i\omega t} = \bar{\bar{w}}_g e^{i\omega t} \quad (54)$$

where

$$\bar{\bar{u}}_g e^{i\omega t} = -\omega^2 \bar{u}_g$$
$$\bar{\bar{w}}_g e^{i\omega t} = -\omega^2 \bar{w}_g \quad (55)$$

The quantities $\bar{\bar{u}}_g$ and $\bar{\bar{w}}_g$ represent the amplitude of the ground acceleration. Therefore equations (34) and (43)

may be expressed in terms of $\bar{\ddot{u}}_g$ and $\bar{\ddot{w}}_g$ as

$$H_u = -\frac{\bar{\ddot{u}}_g}{\omega^2}(R_8 + iI_8)$$

$$H_\theta = -\frac{\bar{\ddot{u}}_g}{\omega^2}(R_9 + iI_9)$$

$$H_w = -\frac{\bar{\ddot{u}}_g}{\omega^2}(R_{10} + iI_{10})$$

$$H_i = -\frac{\bar{\ddot{w}}_g}{\omega^2}[(R_8 + R_9) + i(I_8 + I_9)] \quad (56)$$

Now writing the complex amplitudes $\bar{\ddot{u}}_g$ and $\bar{\ddot{w}}_g$, obtained from the forward Fourier transform as

$$\bar{\ddot{u}}_g = R_{11} + iI_{11}$$
$$\bar{\ddot{w}}_g = R_{12} + iI_{12} \quad (57)$$

and the combined equations (38) and (56) yield

$$u = -\frac{1}{\omega^2}(R_{11} + iI_{11})(R_8 + iI_8)e^{i\omega t}$$

$$u_\theta = -\frac{1}{\omega^2}(R_{11} + iI_{11})(R_9 + iI_9)e^{i\omega t}$$

$$w = -\frac{1}{\omega^2}(R_{12} + iI_{12})(R_{10} + iI_{10})e^{i\omega t}$$

$$u_i = -\frac{1}{\omega^2}(R_{11} + iI_{11})[(R_8 + R_9) + i(I_8 + I_9)]e^{i\omega t} \quad (58)$$

or

$$u = -\frac{1}{\omega^2}(R_{13} + iI_{13})e^{i\omega t}$$

$$u_\theta = -\frac{1}{\omega^2}(R_{14} + iI_{14})e^{i\omega t}$$

$$w = -\frac{1}{\omega^2}(R_{15} + iI_{15})e^{i\omega t}$$

$$u_i = -\frac{1}{\omega^2}(R_{16} + iI_{16})e^{i\omega t} \quad (59)$$

where

$$R_{13} = (R_8R_{11} - I_8I_{11}); \quad I_{13} = (R_{11}I_8 + R_8I_{11})$$
$$R_{14} = (R_9R_{11} - I_9I_{11}); \quad I_{14} = (R_{11}I_9 + R_9I_{11})$$
$$R_{15} = (R_{10}R_{12} - I_{10}I_{12})$$
$$I_{15} = (R_{12}I_{10} + R_{10}I_{12})$$
$$R_{16} = [R_{11}(R_8 + R_9) - I_{11}(I_8 + I_9)]$$
$$I_{16} = [R_{11}(I_8 + I_9) + I_{11}(R_8 + R_9)] \quad (60)$$

The responses u, u_θ, w and u_i in equation (59) represent the component of total response at frequency ω, and hence the complete transient response records are obtained by taking their inverse Fourier transform shown in equation (52). This has been evaluated in discrete form by substituting for $H(\omega)c(\omega)\exp(i\omega t)$ from equation (59). The acceleration response can be obtained by differentiating equations (59) twice and the transient response $\ddot{u}(t)$, $\ddot{u}_\theta(t)$, $\ddot{w}(t)$ and $\ddot{u}_i(t)$ evaluated by taking its inverse Fourier transform.

Input ground motion

The two digitized acceleration records, corrected using the parabolic base line correction technique[1], are used in the present studies. These records are El-Centro, 18 May 1940 and Koyna, 11 December 1967 (longitudinal and vertical components).

For the purpose of computing the vertical displacement response due to the El-Centro earthquake, 100% of the N–S component is assumed to be acting in the vertical direction. *Table 1* lists the earthquake records used in the analysis, together with their associated maximum ground acceleration, velocity and displacement. The latter pair of values have been obtained from the associated ground velocity and displacement records, computed by numerical integration of the corrected acceleration data. A complete set of acceleration time histories of the records employed is presented in *Figures 2* and *3*.

The El-Centro earthquake record has been widely used in earthquake response analysis, and amongst existing records it represents one of the most severe combinations of strong-motion ground acceleration over a long duration. For these reasons, the El-Centro record has

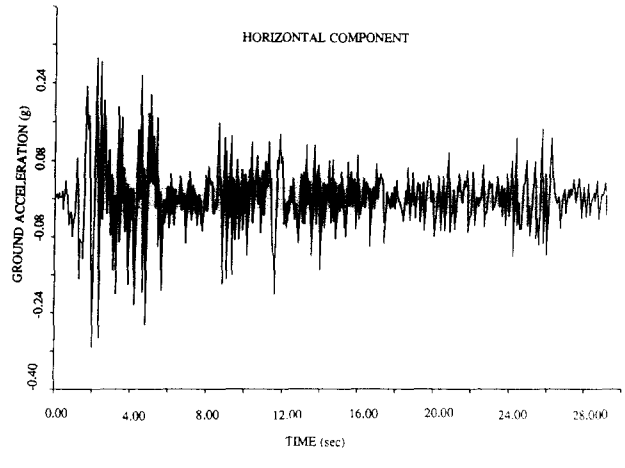

Figure 2 Corrected accelerogram for El-Centro NS 18 May 1940

Table 1

Earthquake record	Component	Date	Maximum ground acceleration (g)	Maximum ground velocity (cm/s)	Maximum ground displacement (cm)	Approximate ground motion (s)
El-Centro	NS	18 May 1940	0.312	32.48	20.91	30.0
Koyna[4]	Longitudinal	11 December 1967	0.631	24.19	13.30	10.3
Koyna[4]	Vertical	11 December 1967	0.341	25.58	28.84	10.3

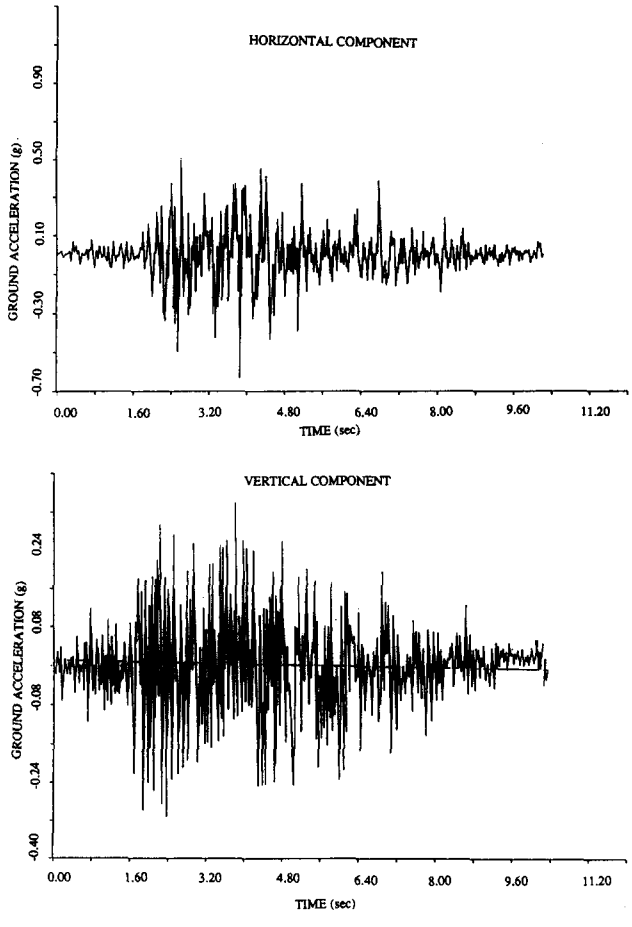

Figure 3 Corrected accelerogram for Koyna 11 December 1967

been chosen along with the Koyna record whose digitized data for horizontal as well as vertical components are available in the literature[4].

Modal response analysis

In the present investigation the individual response quantities are computed separately as a complete time-history; the response maxima u_{max}, $u_{\theta_{max}}$ and w_{max} are then selected from each record as appropriate. The same is true of the combined response ($u_i = u + u_\theta$) whose time history (the sum of the individual time-histories u, u_θ) is computed prior to selecting the maximum response $u_{i_{max}}$.

The maximum displacement responses u_{max}, $u_{\theta_{max}}$, w_{max} and $u_{i_{max}}$, computed for each of the earthquake records, are presented in normalized form in *Figures 4–11*. In each figure, the translational, torsional, combined (u_i) and vertical response curves are shown, normalized to the maximum quantity in the earthquake ground motion records. The resultant horizontal and vertical (u_i and w) response curves are shown in *Figures 12* and *13*. In all cases the responses are plotted as a function of the uncoupled translational and vertical natural periods, T_U and T_W, in the range $0.1 < T_U < 2.0$ s. Five percent damping ($\zeta = 0.05$) is assumed throughout. The horizontal response curves are obtained for three values of eccentricity ratios ($e_r = 0.05$, 0.15 and 0.30) and three values of frequency ratios ($\lambda_T = 0.6$, 1.0 and 1.4), separately. The vertical response curves are also obtained

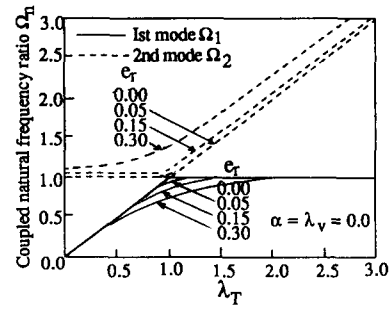

Figure 4 Effect of λ_T and e_r on natural frequencies of torsionally coupled building

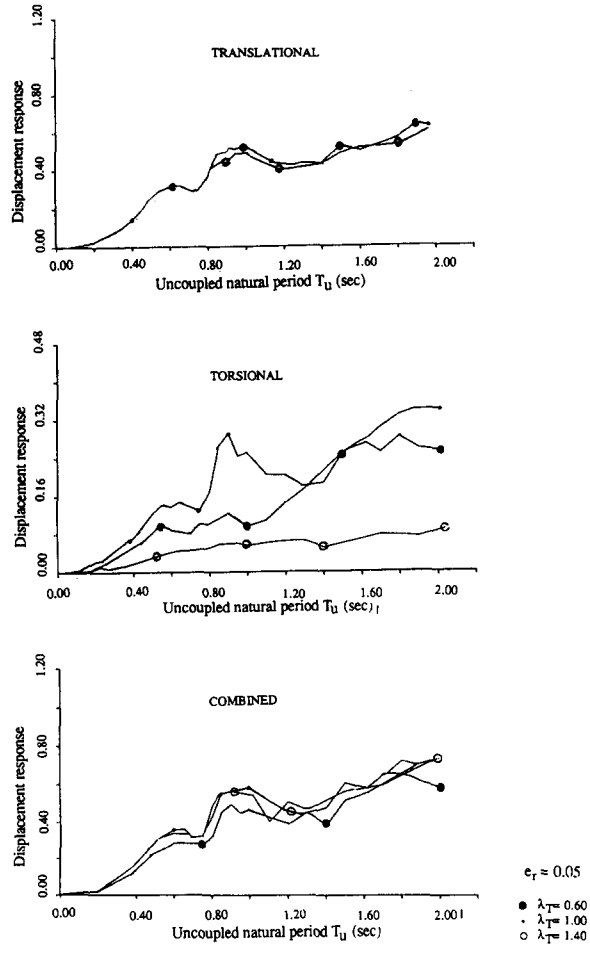

Figure 5 Normalized horizontal displacement response spectra subjected to El Centro earthquake ($e_r = 0.05$)

for the same three values of frequency ratios ($\lambda_v = 0.6$, 1.0 and 1.4) and zero eccentricity in the vertical direction.

Results

Using equation (22) the influence of various parameters, namely α, λ_v, λ_T, e_r, on the natural frequency response of the torsionally coupled building has been evaluated (*Table 2*). *Figure 4* shows the variation of Ω_1 and Ω_2 by varying λ_T and e_r ($\alpha = \lambda_v = 0$) and compared with the results obtained elsewhere[5–7] which are found to be in complete agreement.

In the present analysis it is assumed that the earthquake ground acceleration input in horizontal and verti-

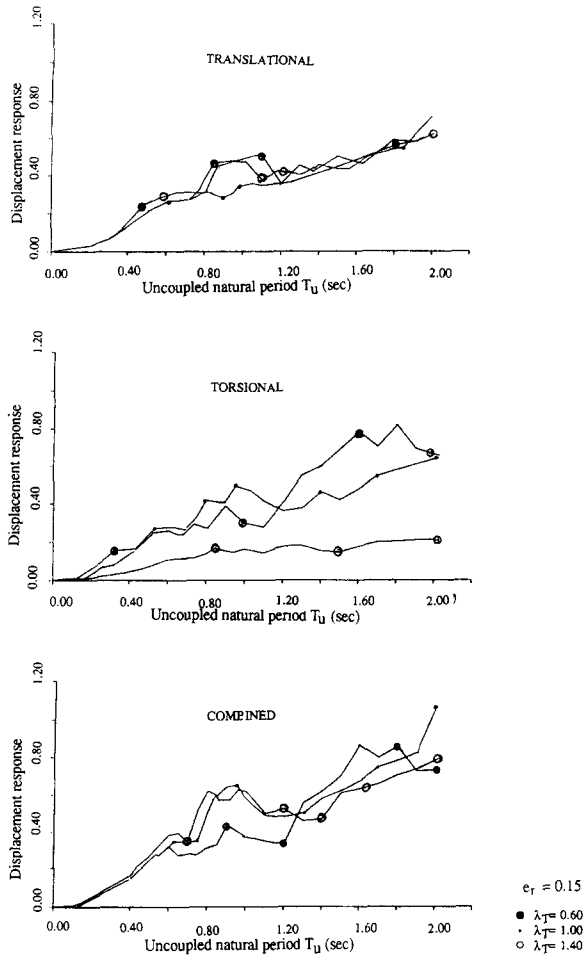

Figure 6 Normalized horizontal displacement response spectra subjected to El Centro earthquake ($e_r = 0.15$)

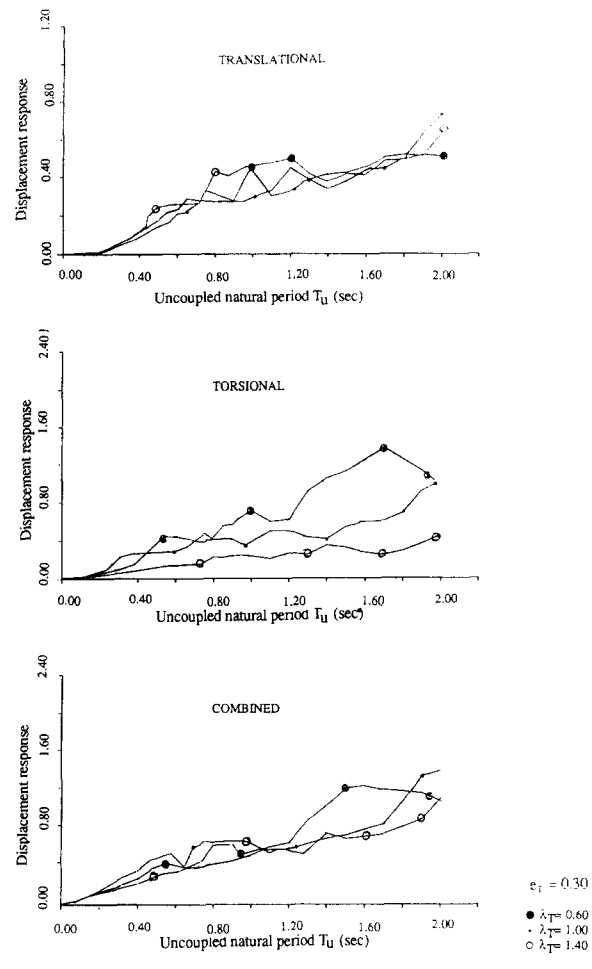

Figure 7 Normalized horizontal displacement response spectra subjected to El Centro earthquake ($e_r = 0.30$)

Table 2

α	λ_v	λ_T	e_r	Natural frequency Ω_1	Ω_2	Ω_3
1	2	3	4	5	6	7
0.0	0.0	0.00	0.05	0.00	1.00	—
			0.15	0.00	1.03	—
			0.30	0.00	1.10	—
		0.05	0.05	0.50	1.00	—
			0.15	0.50	1.03	—
			0.30	0.48	1.13	—
		1.00	0.05	0.96	1.04	—
			0.15	0.91	1.13	—
			0.30	0.84	1.32	—
		1.50	0.05	0.99	1.51	—
			0.15	0.98	1.56	—
			0.30	0.94	1.75	—
		2.00	0.05	1.00	2.01	—
			0.15	0.99	2.06	—
			0.30	0.97	2.27	—
		2.50	0.05	1.00	2.50	—
			0.15	0.99	2.57	—
			0.30	0.98	2.81	—
		3.00	0.05	1.00	3.01	—
			0.15	0.99	3.08	—
			0.30	0.98	3.35	—

cal directions, shown in *Figures 2* and *3*, are applied uniformly over the base of the structure. The structure is modelled to be resting on a rigid foundation, hence interaction effects are neglected. Each of the responses u, u_θ, w and u_i, identified earlier, is evaluated in terms of the time history displacement for a particular earthquake excitation. The calculation is carried out in the frequency domain employing the FFT technique to evaluate the transient responses. The complex frequency response functions H_u, H_θ, H_w and H_i ($= H_u + H_\theta$) are evaluated in discrete form from the solution of equation (27). The derived earthquake responses depend on the structural parameters e_r, λ_T, λ_v, α and ζ together with the translational natural period T_U of the corresponding uncoupled model, as well as the earthquake records. The damping ratio ζ has been taken as 5% of critical damping and the effect of the mass of the vertical elements (columns) of the building is found to be negligibly small and hence neglected ($\alpha = 0$).

The maximum displacement responses u_{max}, $u_{\theta_{max}}$ and $u_{i_{max}}$, normalized to the maximum ground displacement of the horizontal component of the relevant earthquake records, are presented in *Figures 5–10*. These figures show the displacement curves for the El-Centro and Koyna earthquakes for a system with eccentricity ratios $e_r = 0.05$, 0.15 and 0.30 and for three selected values of torsional frequency ratios $\lambda_T = 0.60$, 1.0 and 1.4. The following trends are observed.

The vertical response is obtained for three different values of frequency ratios ($\lambda_v = 0.6$, 1.0 and 1.4). The vertical eccentricity is zero as the mass of the vertical elements (columns) of the building (α) is lumped in line with the centre of resistance. The maximum displacement

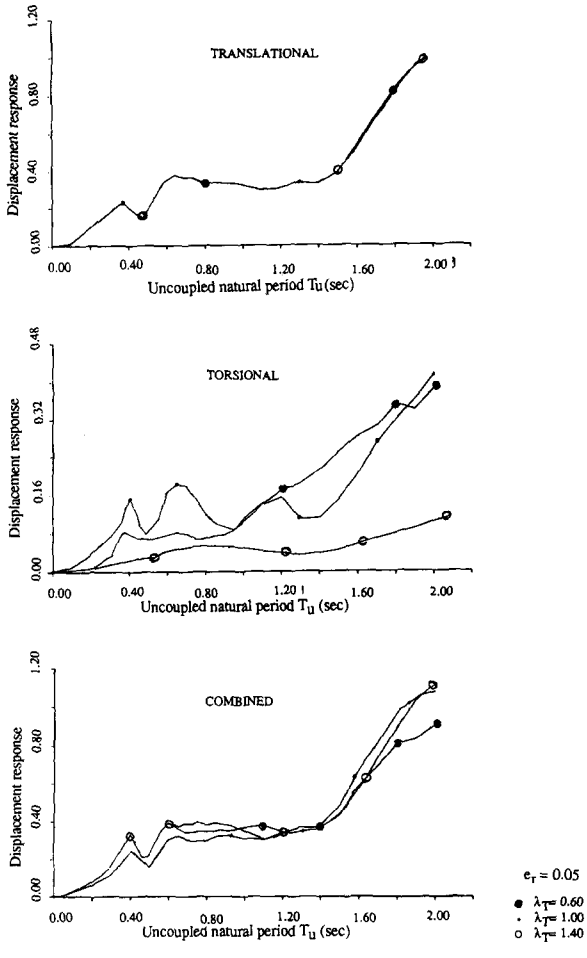

Figure 8 Normalized horizontal displacement response spectra subjected to Koyna earthquake ($e_r = 0.05$)

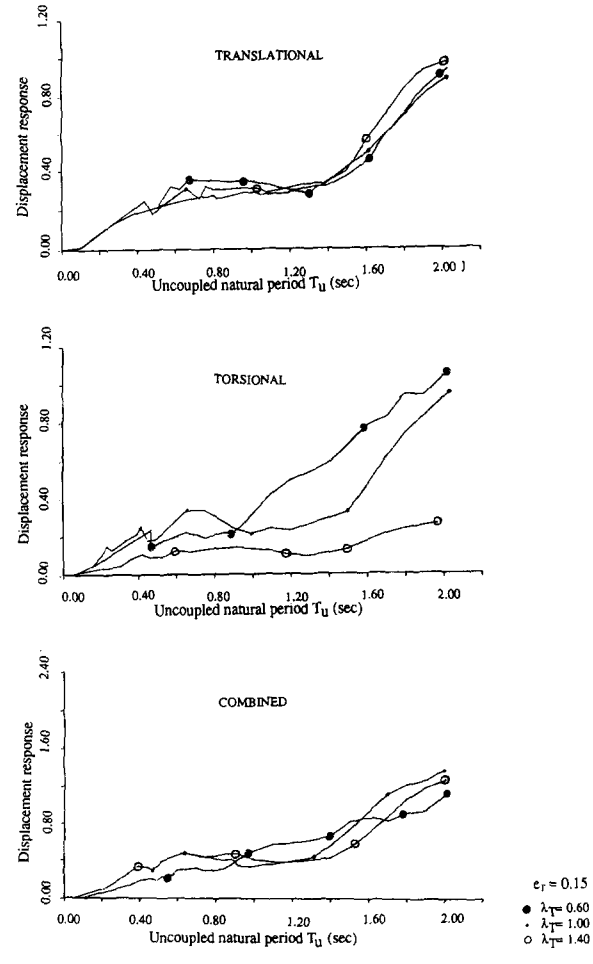

Figure 9 Normalized horizontal displacement response spectra subjected to Koyna earthquake ($e_r = 0.15$)

response w_{max}, normalized to the maximum ground displacement of the vertical component of the relevant earthquake records, are presented in *Figures 11* and *12*. The resultant response is obtained by using equation (49) for three different values of eccentricity ratios ($e_r = 0.05$, 0.15 and 0.30). For each eccentricity ratio value the response is obtained for three different values of vertical frequency ratios ($\lambda_v = 0.6$, 1.0 and 1.4) and are presented in *Figures 13* and *14*.

El-Centro output

Horizontal response (Figures 5–7)

Small eccentricity ratio ($e_r = 0.05$)

(i) The translational displacement curves are quite close to each other for all λ_T values in the entire range of T_U (0.0–2.0 s). The response increases when T_U lies between 0.80 s and 1.0 s. There is a gradual increase of response from $T_U = 1.20$ to 2.0 s.

(ii) The torsional response for $\lambda_T = 0.6$ increases gradually from $T_U = 1.0$ s to 1.6 s and afterwards becomes almost steady. For $T = 1.0$, it exceeds the earlier value by about a factor of 2.0 at $T_U = 0.9$ s and is higher between $T_U = 1.6$ s to 2.0 s. For $\lambda_T = 1.4$, the displacement response is very much lower than the earlier two curves during the entire range of T_U.

(iii) The combined response for $\lambda_T = 0.6$ increases gradually producing a hump at $T_U = 0.9$ s. The maximum value is obtained at $T_U = 1.8$ s. For $\lambda_T = 1.0$ and 1.4, the responses are higher over the entire range of T_U.

Intermediate eccentricity ratio ($e_r = 0.15$)

(i) The translational response trend is about the same as for small eccentricities ($e_r = 0.05$) for all values of λ_T except that the response corresponding to $\lambda_T = 1.0$ is much lower than the response for $\lambda_T = 0.6$ and 1.4 in the range of T_U between 0.80 s and 1.20 s. The response for $\lambda_T = 1.0$ exceeds the other two at $\lambda_T = 2.0$.

(ii) The torsional response for $\lambda_T = 0.6$ is lower than for $\lambda_T = 1.0$ until $T_U = 1.2$ s. When $T_U > 1.2$ s, this exceeds the response corresponding to $\lambda_T = 1.0$. The response for $\lambda_T = 1.40$ is much lower than the other two and similar to the one for small eccentricity ratio ($e_r = 0.05$) but higher in values.

(iii) The combined response for $\lambda_T = 0.6$ is lower than the responses corresponding to $\lambda_T = 1.0$ and 1.4 until $T_U = 1.3$ s and exceeds them when T_U lies between 1.3 s and 1.9 s. It again becomes lower than any other two at $T_U = 2.0$ s. The responses corresponding to $\lambda_T = 1.0$ and 1.4 exceeds the response for $\lambda_T = 0.6$ until $T_U = 1.3$ s and afterwards they become lower when T_U lies between 1.3 s and 1.9 s. The combined response exceeds them at $T_U = 2.0$.

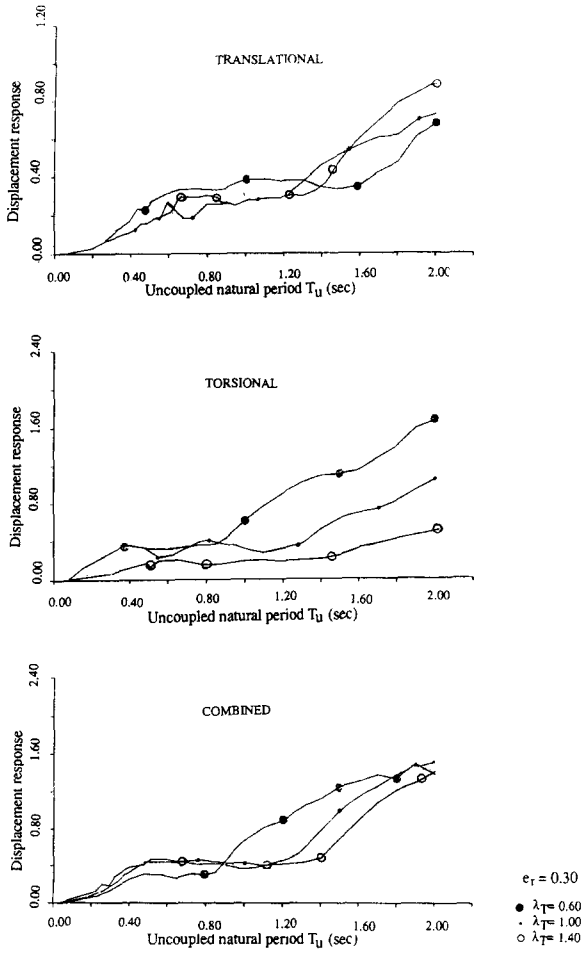

Figure 10 Normalized horizontal displacement response spectra subjected to Koyna earthquake (e_r = 0.30)

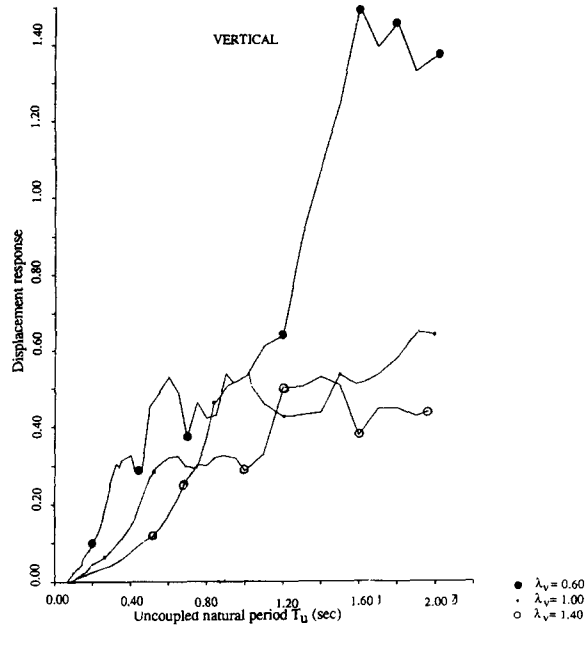

Figure 11 Normalized vertical displacement response spectra subjected to El Centro earthquake (λ_v = 0.6, 1.0, 1.4)

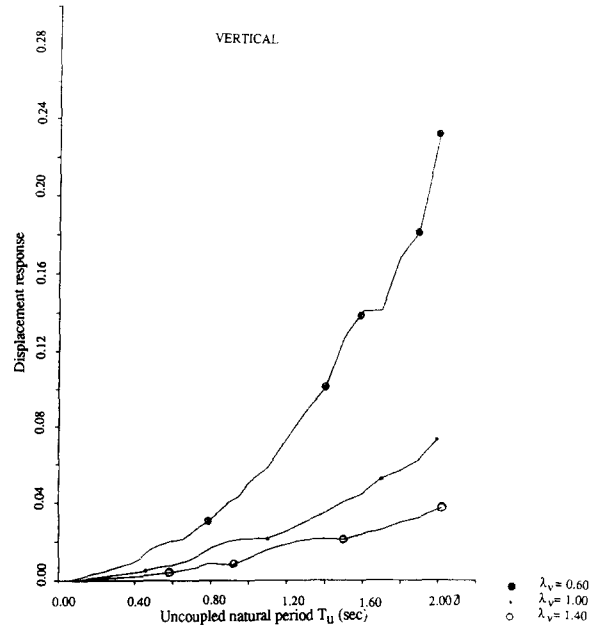

Figure 12 Normalized vertical displacement response spectra subjected to Koyna earthquake (λ_v = 0.6, 1.0, 1.4)

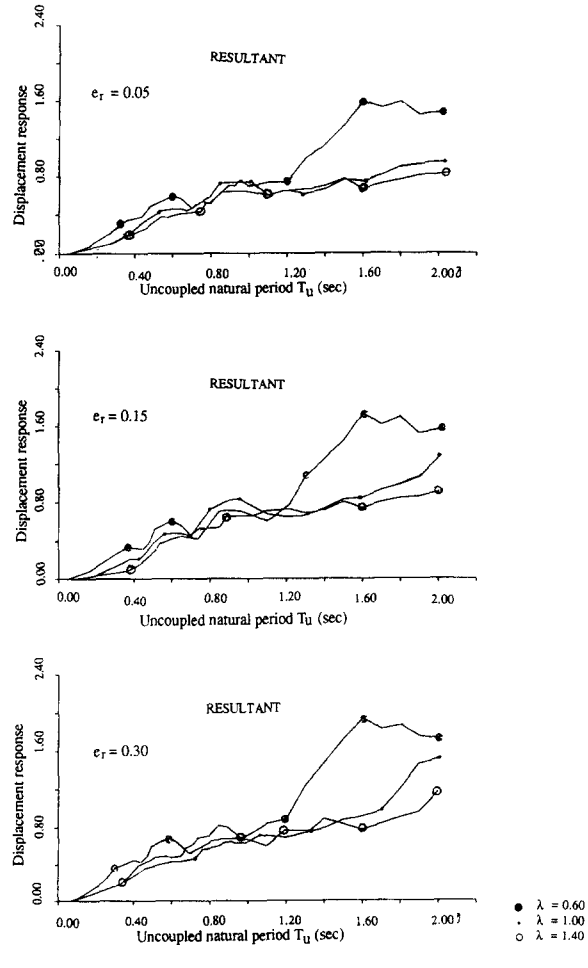

Figure 13 Normalized resultant displacement response spectra subjected to El Centro earthquake (e_r = 0.05, 0.15, 0.30)

Large eccentricity (e_r = 0.30)

(i) The translational response for $\lambda_T = 0.6$ exceeds the other two curves corresponding to $\lambda_T = 1.0$ and 1.4 in the T_U range between 1.0 s and 1.2 s and is lower when $T_U > 1.7$ s. There is a hump in the response curve for $\lambda_T = 1.4$ when T_U lies between 0.8 s and 1.0 s. The response curve corresponding to $\lambda_T = 1.4$ increases gradually after $T_U = 1.8$ s.

(ii) The torsional response curve corresponding to $\lambda_T = 0.6$ exceeds the other two curves for $\lambda_T = 1.0$

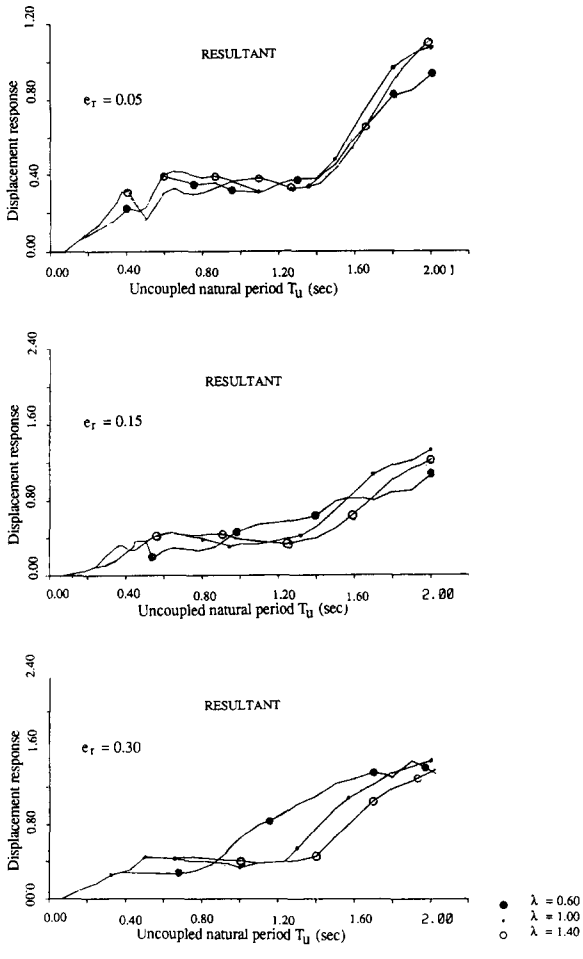

Figure 14 Normalized resultant displacement response spectra subjected to Koyna earthquake (e_r = 0.05, 0.15, 0.30)

and 1.4 over almost the entire range of T_U. As the frequency ratio (λ_T) values increase, the response values become lower over the whole range of T_U. The minimum response is obtained for the highest value of $\lambda_T = 1.4$.

(iii) The combined response corresponding to $\lambda_T = 0.6$ is more than the responses for $\lambda_T = 1.0$ and 1.4 when $1.2 < T_U < 1.8$. The response curves corresponding to $\lambda_T = 1.0$ and 1.4 run quite close to each other making a hump at $0.6 < T_U < 1.0$ s.

Vertical response (Figure 11)

(i) The response curve corresponding to $\lambda_v = 0.6$ exceeds the other two response curves for $\lambda_v = 1.0$ and 1.4 over the entire range of T_U values. There is a sharp increase when $T_U > 1.2$ s.

(ii) The response curve corresponding to $\lambda_v = 1.0$ is lower than the curve for $\lambda_v = 0.6$ throughout the entire range of T_U. When $T_U > 1.2$ s, the response difference has a factor of greater than 2.

(iii) The response curve corresponding to $\lambda_v = 1.4$ is lower than the curve for $\lambda_v = 1.0$ except for $1.1 < T_U < 1.4$. The response is also quite sensitive to λ_v at lower values of T_U.

Resultant response (Figure 13) $\lambda_T = \lambda_v = \lambda$

(i) The response curves for $\lambda = 1.0$ and 1.4 run quite close to each other over the entire range of T_U. The curve corresponding to $\lambda = 0.6$ closely follows the other two curves until $T_U = 1.2$ and exceeds them when $1.2 < T_U < 2.0$. In this range the response exceeds them by a factor of approximately 2.0. This trend is observed in all three sets of e_r values that are considered.

(ii) The maximum response is obtained at $T_U = 1.6$ s.

(iii) The difference between the responses for $\lambda = 1.0$ and 1.4 increases at $T_U = 2.0$ as the e_r value increases.

Koyna output

Horizontal response (Figures 8–10)

Small eccentricity ($e_r = 0.05$)

(i) The translational response curves for $\lambda_T = 0.6$, 1.0 and 1.4 almost overlaps each other in the entire range of T_U. The curves start gradually, make a dip at $T_U = 0.45$ s, stay constant between $0.6 < T_U < 1.4$ and start gradually increasing. The higher response is obtained at higher values of T_U.

(ii) The torsional response curve for $\lambda_T = 0.6$ is almost flat until $T_U = 1.0$ s and then increases gradually with T_U exceeding the response curve corresponding to $\lambda_T = 1.0$ which forms a dip at $T_U = 1.4$ s. This curve forms a hump at $0.5 < T_U < 0.7$ and exceeds the first one in value until $T_U = 1.0$ s. The response curve corresponding to $\lambda_T = 1.4$ is lower than the other two over the entire range of T_U. The higher response is obtained for smaller λ_T and higher T_U values.

(iii) The combined response curves for $\lambda_T = 0.6$, 1.0 and 1.4 run quite close to each other over the entire range. The general pattern is like the translational response curves because the influence of the torsional response is small.

Intermediate eccentricity ($e_r = 0.15$)

(i) The translational response curves for $\lambda_T = 0.6$, 1.0 and 1.4 show variation in values over the curves for small eccentricity ($e_r = 0.05$) but maintain the same pattern. The higher values are obtained for $\lambda_T = 1.4$ when $T_U = 1.6$ s.

(ii) The torsional response curves for $\lambda_T = 0.6$, 1.0 and 1.4 show the influence of eccentricity maintaining the same pattern as for small eccentricity ($e_r = 0.05$).

(iii) The combined response curves for $\lambda_T = 0.6$, 1.0 and 1.4 indicate the influence eccentricity maintaining the same pattern as for small eccentricity ($e_r = 0.05$). The higher values are obtained for the curve $\lambda_T = 1.0$ when $T_U > 1.6$ s.

Large eccentricity ($e_r = 0.30$)

(i) The translational response curve corresponding to $\lambda_T = 0.6$ increases gradually, stays flat between $0.6 < T_U < 1.6$ and then increases gradually until $T_U = 2.0$ s which exceeds the other two curves for $\lambda_T = 1.0$ and 1.4 until $T_U = 1.2$ and stays lower after $T_U > 1.2$ s. The higher response is obtained for the curve $\lambda_T = 1.4$ when $T_U > 1.6$ s.

(ii) The torsional response is higher than the translational response due to large eccentricity. The higher response is obtained for the smaller frequency ratio ($\lambda_T = 0.6$) which reduces for larger λ_T values throughout almost the entire range of T_U.

(iii) The combined response curve for $\lambda_T = 0.6$ shows lower values than the curves for $\lambda_T = 1.0$ and 1.4 when $T_U < 0.8$. This curve exceeds the other two when $T_U > 0.8$ s.

Vertical response (Figure 12)

(i) The response curves increase in magnitude with T_U values.
(ii) The maximum response is obtained for lower values of the frequency ratio ($\lambda_v = 0.6$) and smaller response values are obtained for the higher frequency ratio ($\lambda_v = 1.4$).
(iii) The frequency ratio (λ_v) values are very sensitive to the response. The maximum response for $\lambda_v = 0.6$ is about 4 times higher than the maximum response for $\lambda_T = 1.0$ at $T_U = 2.0$ s.

Resultant response (Figure 14) $\lambda_T = \lambda_v = \lambda$

(i) For a small eccentricity ratio ($e_r = 0.05$) the resultant curves for $\lambda = 0.6$, 1.0 and 1.4 run quite close to each other and higher values are obtained when $T_U > 1.4$ s. The response curves for higher λ values show a higher response.
(ii) For an intermediate eccentricity ratio ($e_r = 0.15$) the resultant curves for $\lambda = 0.6$, 1.0 and 1.4 show variations and produce higher values for $\lambda = 0.6$ between $1.0 < T_U < 1.6$ s. The higher response between $1.6 < T_U < 2.0$ is obtained due to $\lambda = 1.0$.
(iii) For a large eccentricity ratio ($e_r = 0.30$) the resultant curves for $\lambda = 0.6$, 1.0 and 1.4 show variations and produce higher values for $\lambda = 0.6$ between $0.9 < T_U < 2.0$ s. The other two curves show lower values in this range of T_U.

Conclusions

(1) The horizontal response ($= u + u_\theta$) increases more rapidly when $T_U > 1.4$ s.
(2) The effect of larger eccentricity (e_r) is to increase the translational response (u) for smaller frequency ratios (λ_T).
(3) The torsional response (u_θ) increases significantly when the eccentricity ratio (e_r) is increased.
(4) For a larger eccentricity ratio (e_r) the torsional response (u_θ) may exceed the translational response (u).
(5) The vertical response (w) is very sensitive to the frequency ratio (λ_v) values. For smaller λ_v values, the response is much higher when $T_U > 1.2$ s.
(6) The resultant response ($\bar{X}_i$) increases when $T_U > 1.2$ s.
(7) The influence of higher eccentricity ratio (e_r) is to increase the resultant response for smaller frequency ratios (λ).
(8) The magnitude of response depends upon the maximum ground displacement. The maximum displacement response, computed for each of the earthquake records, are normalized to the maximum quantity in the earthquake ground motion records.

References

1 Schiff, A and Bogdanoff, J. L. 'Analysis of current methods of interpreting strong motion accelerograms,' *Bull. Seism. Soc. Amer.* 1967, **57**(5), 857–874
2 Cooley, J. W. and Tukey, J. W. 'An algorithm for machine calculation of complex Fourier series,' *Maths Comput.* 1965, **19**, 297–301
3 Hall, J. F. 'An FFT algorithm for structural dynamics,' *Earthquake Engng Struct. Dyn.* 1982, **10**, 797–811
4 Krishna, J., Chandrasekaran, A. R. and Saini, S. S. 'Analysis of Koyna accelerogram of December 11, 1967,' *Bull. Seism. Soc. Amer.* 1969, **59**(4), 1719–1731
5 Chandler, A. M. and Hutchinson, G. L. 'Evaluation of Code torsional provisions by a time history approach,' *Earthquake Engng Struct. Dyn.* 1987, **15**, 491–516
6 Tsicnias, T. G. and Hutchinson, G. L. 'Evaluation of code requirements for the earthquake resistant design of torsionally coupled buildings,' *Proc. Instn Civ. Engrs*, Part 2 1981, **71**, 821–843
7 Chandler, A. M. and Hutchinson, G. L. 'Torsional coupling effects in the earthquake response of asymmetric buildings,' *Engng Struct.* 1986, **8**, 222–237